4.1 Introduction

The present chapter describes the synthesis of magnesium alloy composite specimens and their characterization using different techniques. A flow chart showing synthesis of the composite via powder metallurgy route is mentioned in Fig. 4.1.

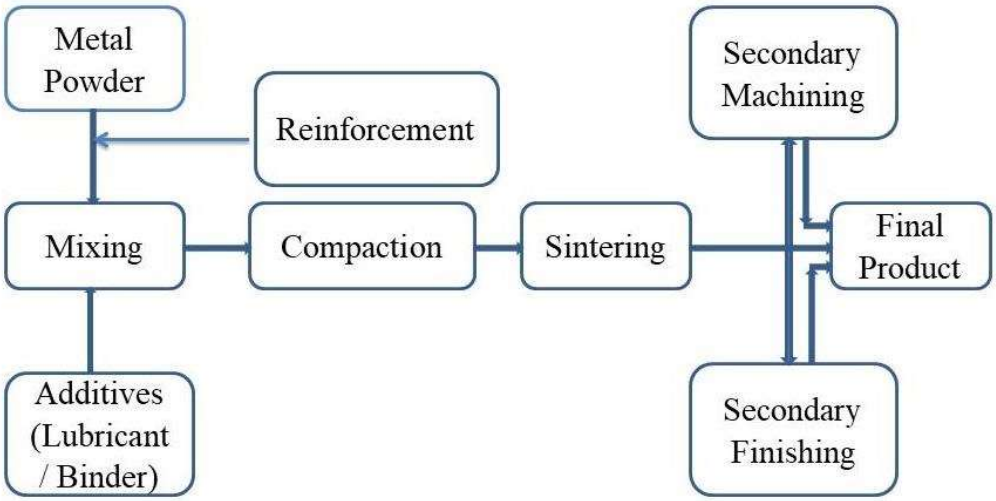

FIGURE 4.1: Flow diagram for synthesis of different composites by powder metallurgy route

4.2. Preparation of magnesium-based alloy and composites

The composites were prepared by using magnesium alloy as matrix and addition of hydroxyapatite powder, and bioactive glasses of different types. The method of preparation of magnesium alloy and the bioactive glass is mentioned below.

4.2.1 Preparation of magnesium alloy

The magnesium-based alloy was prepared by powder metallurgy route as shown in steps mentioned in Fig. 4.1. The raw materials and the methods adopted to prepare the composites are discussed in subsequent sections. The magnesium alloys used in the present work were consists of two compositions as shown in Table 4.1. The alloys were further used as base materials and then reinforced with different materials.

TABLE 4.1: Composition of base alloys

S.N	Alloy	Magnesium (wt%)	Zinc (wt%)	Manganese (wt%)	Aluminum (wt%)	Calcium (wt%)
1.	Mg20Zn2Mn	77.91	20.07	2.02	nil	nil
2.	Mg3Al2Zn0.6Ca	94.5	2	nil	3	0.6

4.2.2 Preparation of HAp

Hydroxyapatite was prepared by using pure Calcium Hydroxide ($Ca(OH)_2$) and Ammonium Hydrogen Phosphate ($(NH_4)_2HPO_4$). The powders were mixed in the ratio so as to maintain the Ca/P ratio in apatite as 1.67.

Following are the steps followed for the preparation of Hydroxyapatite according to VK Singh and B. Ravindra Reddy (V.K. Singh and B. R. Reddy, 2012).

Steps:

1. 0.6 M $(NH_4)_2HPO_4$ solution was prepared by adding 19.8 gm./250 ml of distilled water.

2. Also, 1M $Ca(OH)_2$ solution was prepared by adding 18.5 gm./250 ml of distilled water.

3. Now both the stock solutions were mixed appropriately on a magnetic stirrer for 1.5 hrs until the pH is maintained at 9.75.

4. Filtrate was taken out after at least 6-7 filtrations using the filter paper. The equilibrium reaction between the reagents is as follows:

$$10\ Ca(OH)_2 + 6\ (NH_4)_2HPO_4 \longrightarrow Ca_{10}(PO_4)_6.(OH)_2 + 12NH_4OH + 6H_2O \qquad (4.1)$$

5. The filtrate was kept in an oven at 150°C for drying for at least 20 hrs.

6. Further, the dried powder was taken out and kept in a furnace at 900°C for 1hr for calcination process with a heating rate of 10°C and a holding time of 1 hr.

4.2.3 Preparation of S45P7 BAG

The bioactive glass was prepared by the melt-quench technique. The components used for preparation of the S45P7 BAG were 46.6 % SiO_2, 24.1 % Na_2O, 24.4 % CaO, 3% P_2O_5 and 2 % B_2O_3. These were thoroughly mixed and further melted at sufficient temperature and hence quenched in water to get desired results.

Following are the preparatory steps followed in order to develop required bioactive glass (W. Huang, et al. 2006):

1. All powders were mixed thoroughly on a ball mill at an RPM of about 100 rpm using zirconia balls of 10 mm size for about 5 hrs to get a homogenized mixture. The ball powder ratio was taken as 20:1.

2. Now the powdered sample was kept in a furnace at 1150°C with a heating rate of 10°C and a holding time of at least 5 hrs and then quenched in a water bath.

3. Further, the quenched sample was crushed thoroughly using a mortar and pestle.

4. Further the sample was given for spectroscopic analysis.

5. Also the sample was kept in an SBF solution for 0, 7, and 14 days to investigate its bio-active nature.

4.2.4 Preparation of 1393 BAG

The 1393 BAG used in the present study were prepared by mixing the following reagent with weight percentage: 6% Na2O, 20% CaO, 12% K2O, 5% MgO, 4% P_2O_5 and 53% SiO_2 using a pestle and mortar (A. Hoppe, et al. 2014). The mixed reagents were melted in a platinum crucible at 1400 °C in the electric furnace and quenched in water. The glass was crushed and was ball milled in the pot mill to bring in the powder form.

4.3 Processing of raw materials to prepare different composites

The alloys of different compositions as discussed earlier were reinforced with reinforcement such as HAp, S45P7 BAG and 1393 BAG. The processing of the composites was done as explained below.

4.3.1 Raw Materials

The major constituents used in the preparation of magnesium-based alloys and composites are magnesium, aluminum, zinc, calcium and manganese. In the synthesis, all materials were of analytical grade, and not further purified. The digital images of the powdered raw materials are shown in Fig. 4.2, to Fig. 4.6. Also, the materials, their purity, manufacturing company names and physical properties are listed in Table 4.2.

FIGURE 4.2: Digital image of magnesium powder

FIGURE 4.3: Digital image of zinc powder

FIGURE 4.4: Digital image of aluminum powder

FIGURE 4.5: Digital image of manganese powder

FIGURE 4.6: Digital image of calcium powder

FIGURE 4.7: Digital image of HAp powder

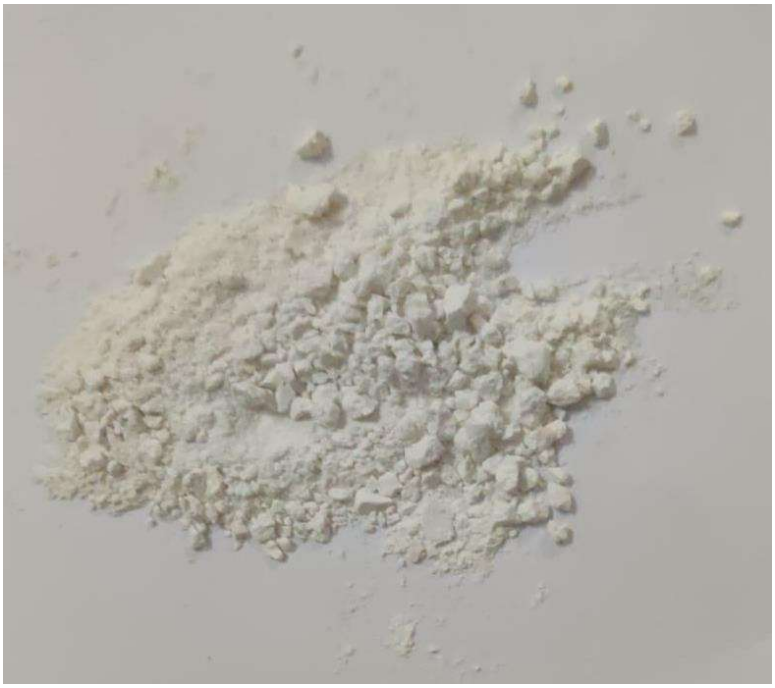

FIGURE 4.8: Digital image of S45P7 BAG

FIGURE 4.9: Digital image of 1393 BAG powder

TABLE 4.2: Characteristics of materials used

S.N	Powder	Supplier	Purity (%)	Density (g/cm^3)	Melting Point (°C)	Boiling Point(°C)
1	Mg	Loba Chemie, Mumbai, India	99.5	1.74	648	1100
2	Al	Loba Chemie, Mumbai, India	98.0	2.7	660.37	2327
3	Zn	Loba Chemie, Mumbai, India	99.5	7.133	420	907
4	Ca	Loba Chemie, Mumbai, India	98.0	1.54	850	1440
5	Mn	Loba Chemie, Mumbai, India	99.0	7.3	1260	1900

4.3.2 Weighing and mixing

The various ingredients used to prepare the magnesium alloy based composites were taken in appropriate percentage and weighed using an electronic balance and was mechanically powdered into small particles using ball mills. For the preparation of powder, grounding of the powder was done with the help of grinding balls in a planetary ball mill. The Image of a laboratory planetary mill is shown in Fig. 4.10.

FIGURE 4.10: Planetary ball mill

In the ball mill, zirconia balls were added as grinding media for better mixing, where The ball powder ratio was taken as 20:1. A ball mill breaks the sample and reduces the powder to a uniform size. It was performed for 4 hours at a speed of 200 rpm and after every 15 minutes of a cycle a halt time of 15 minutes was given to avoid oxidation and 3 weight percent of ethanol was added as anti-agglomerate (A. Nouri, and C. Wen, 2014). The final powder contained a homogenous mixture of all the added powders. The particle size of the powders was estimated by sieve analysis. The average particle size of the base alloy and reinforcement is mentioned in Table no.4.3

TABLE 4.3: Average particle size of base alloy and reinforcement

S.N	Material/Reinforcement	Average Particle Size (µm)
1.	Base alloy	78.33
2.	Hydroxyapatite (HAp)	52.42
3.	S45P7 Bioactive Glass	49.95
4.	1393 Bioactive Glass	54.78

4.3.3 Compaction

After milling, the agglomerate was compressed using a die & punch (Fig.4.11) with the help of hydraulic press (Fig. 4.12) and prepared in various shapes, which were used as a specimen for different testing, viz. pellets (diameter 15 mm and thickness 4 mm), cylinders (d=15mm and l=30mm), bar (25mm×10mm×10mm). The test specimens of the different compositions were prepared with the help of a uni-axial press machine at 200 MPa applied pressure.

FIGURE 4.11: Die and punch assembly for preparation of pellets

FIGURE 4.12: Hydraulic press

4.3.4 Sintering

The green composite was subjected to sintering in an inert gas atmosphere controlled tube furnace at a temperature of 630 °C with a holding time of 1 hour. The rate of heating was kept 100 °C min^{-1}. Magnesium being the highly reactive metal requires special attention during sintering.

4.4 Characterization techniques

Different characterization techniques used for the analysis of various physical, mechanical and chemical properties of the sintered composite and composite specimens are listed in Fig. 4.13.

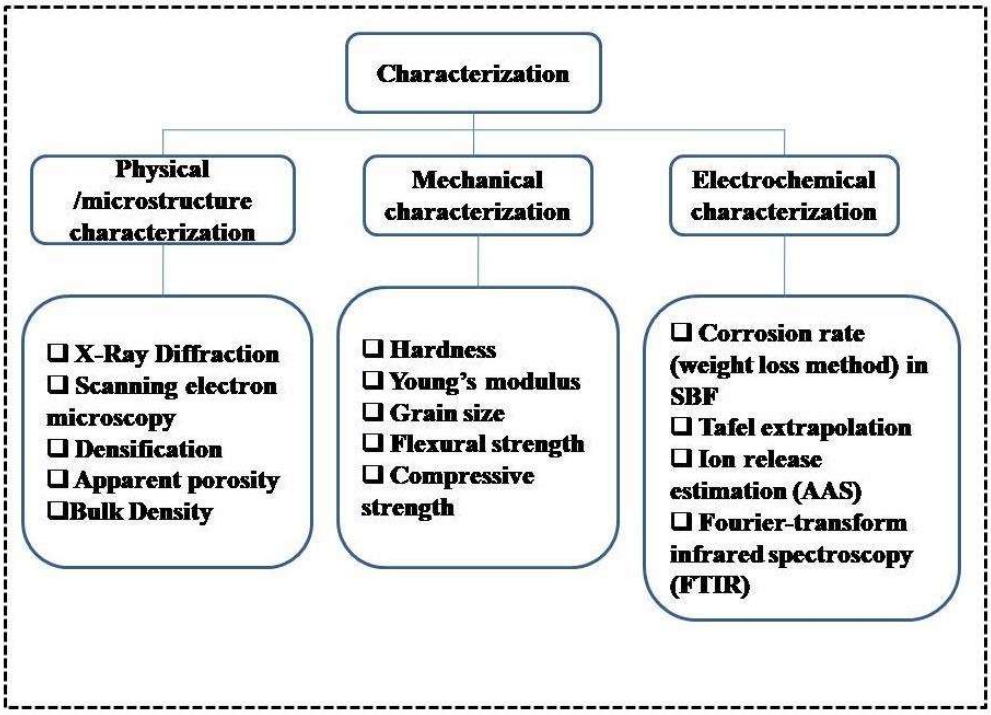

FIGURE 4.13: Different characterizations techniques

4.4.1 Physical/Microstructure characterization

The physical properties and microstructural changes appearing in the composites after sintering were observed by various characterization techniques as mentioned in subsequent subsections.

4.4.1.1 X-ray Diffraction (XRD)

X-ray diffraction is a primary non-destructive analytical technique for the determination of the chemical composition and crystallographic structure of the materials. It is also helpful to determine the lattice parameters, lattice defects, lattice strain, crystallite size, dislocation density and phases of known and unknown materials. It is an electromagnetic wave with a wavelength of the order of one angstrom, and when it is incident upon the sample, diffraction from different atoms takes place. In the crystal, the arrangements of atoms are in a periodic manner, and diffracted x-rays from these atoms form constructive interference and peaks are observed. Therefore, the crystal structure of materials can be determined by measuring the distribution of the diffraction pattern. The inter-planer distance can be calculated according to Bragg's law as given below (B. Cullity, 1956; S. Marchesini, et al. 2003).

$$2d\sin\theta = n\lambda \tag{4.1}$$

Where 'θ' is the incident angle, 'λ' is the wavelength of the x-ray, and 'n' is an integer representing the order of the diffraction. This process is shown schematically in Fig. 4.14, and the experimental setup is shown in Fig. 4.15.

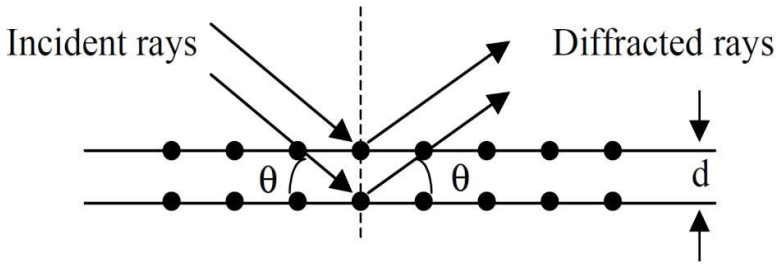

FIGURE 4.14: Schematic of diffraction of X-rays by a crystal.

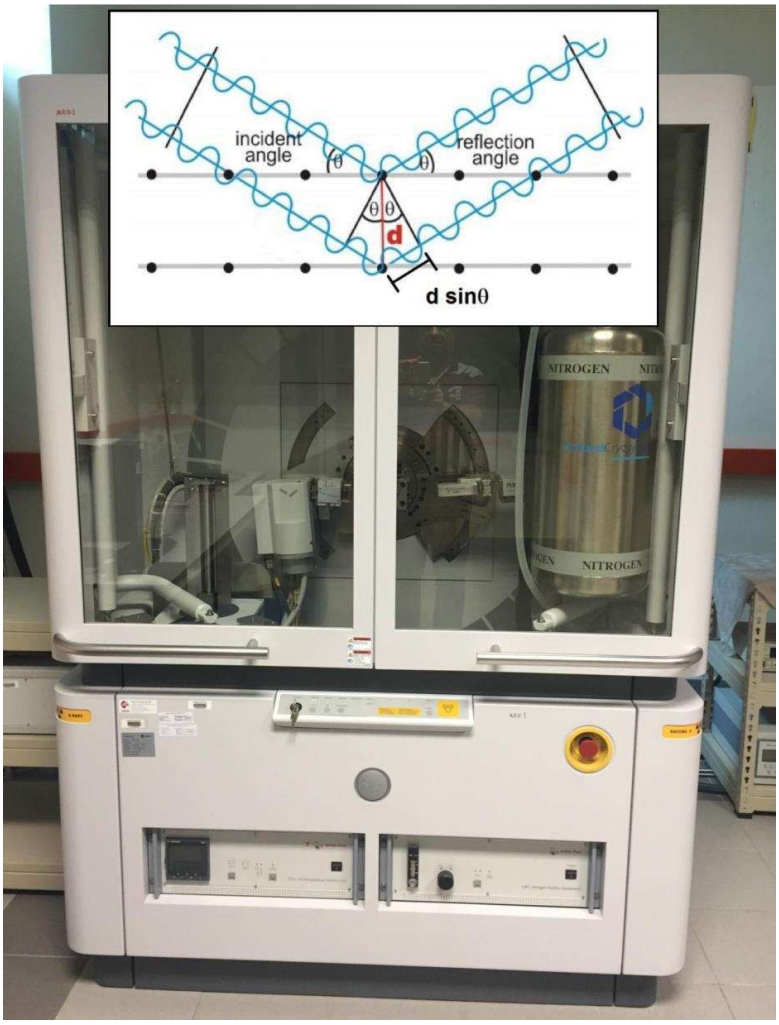

FIGURE 4.15: X-ray diffraction measurement setup

In our study, the phase evolution and structure of the magnesium-based composite were studied by BrukerD8, U.K. X-ray diffraction experiments were performed using an 18 kW rotating anode (CuK_{α}) based Rigaku high-resolution X-ray powder diffractometer, operating in the Bragg-Brentano geometry and fitted with a graphite monochromator in the diffraction beam. The generator was operated at 40KV and 150mA. The powder samples were placed on a grooved quartz sample holder with the help of a glass slide. The diffraction experiments were applied at a fixed wavelength λ, (CuK_{α}= 1.54056A^{o}) and

diffraction angles (2θ) selected were in the range of 10^{o}-$80^{o}$with 5°/min scanning speed. Analysis of the obtained pattern was done with the help of X pert high score software using standard JCPDS files. In the present work, in case of corrosion tests the phases formed after corrosion were also analyzed by the XRD technique after immersion of the samples in corrosive media.

4.4.1.2 Scanning electron microscopy (SEM)

A Scanning electron microscope is used to obtain the surface morphology of a sample at different magnifications, resolution, and depth of focus. The images are taken at a higher resolution as compared to the optical microscope. A well-focused monoenergetic electron beam is incident on the given solid surface. The interaction between beam and the surface results in different scattering processes. Secondary electrons (SE) and backscattered electrons (BSE) are mainly used in the SEM technique to get the surface morphology. This BSE or SE are collected and converted into current signals which are amplified to control the brightness of the cathode ray tube (CRT)/screen of monitor (S. L. Flegler, et al. 1993; P. Kazemian, et al. 2007). SEM works in vacuum conditions. Therefore, special sample preparation is required before putting the samples for imaging. No moisture content should be there in the sample or the chamber because it would inhibit the vacuum in the chamber. Since the sample should be conducting in nature, therefore, metals do not need any preparation before being used. In present work, SEM analysis of all samples sintered and that after formation of corrosion products were done to know the surface morphology and elements present. For microstructure determination, all the samples were polished using emery papers of grades 1/0, 2/0, 3/0 and 4/0 (Sia, Switzerland) followed by

polishing. Samples sintered were etched with the solution: 100ml ethanol, 2ml Hydrochloric Acid to get clear images. The Scanning Electron Micrograph analysis was carried out with the help of the instrument model- INSPECT 50 FEI. Model: EVO - Scanning Electron Microscope MA15 / 18 of Company: CARL ZEISS MICROSCOPY LTD. equipped with energy dispersive spectroscopy (EDX) system. EDX and mapping were recorded at specific magnification to get the elemental analysis of as prepared and corroded surfaces.

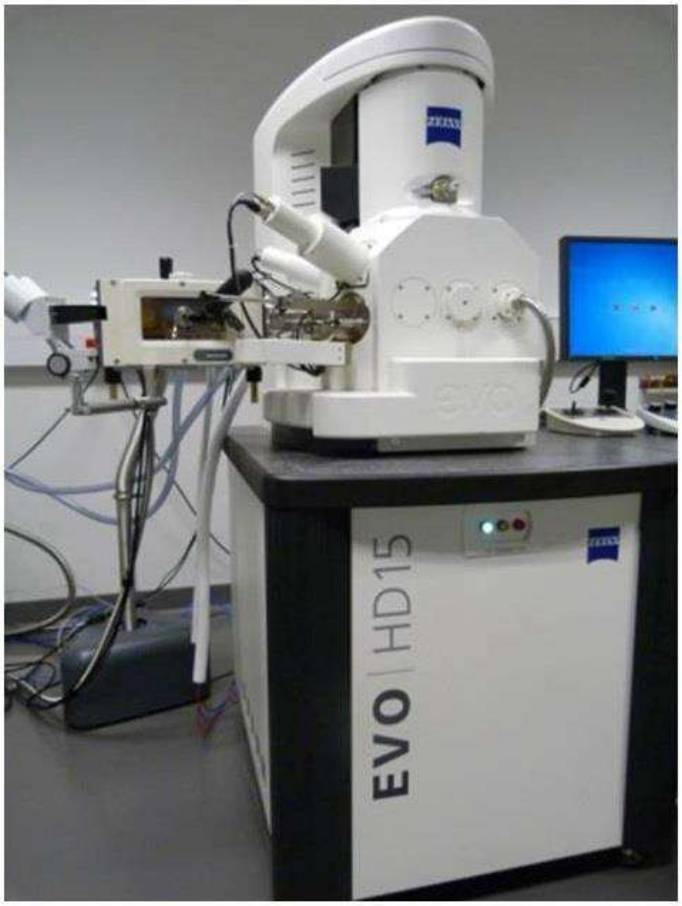

FIGURE 4.16: Scanning electron microscopy setup

4.4.1.3 Actual density, theoretical density and percentage relative density

The actual density of the magnesium-based specimens after sintering was calculated to know the aftermath of sintering on densification. The actual density of the samples was measured with the help of the Archimedes principle (H. H. Rieke III and G.V. Chilingarian) method for measuring the density in which the weight of the samples is measured in air and the liquid used here was water. The weights were measured with an OHAUS AX324 precision balance of 0.1 mg resolution. The dry weight of the samples was measured and then all the sample was suspended in water by using a string, after the emersion, their suspended weight was noted, the following equations were used for measuring the true density.

$$\text{True Density } (g/cm^3) = \frac{D}{D-S} \qquad (4.2)$$

Where S= Suspended weight in grams, D=Dry weight in grams

Also, the theoretical density of the powder samples (three-component system in our case) was calculated by the rule of mixture (S.C. Sharma, 2003) as mentioned below:

$$\text{Theoretical density of mixture, } \rho = (m_1+m_2+m_3)/(V_1+V_2+V_3) \qquad (4.3)$$

Where, m_1, m_2, and m_3 are the weight of the components in grams, V_1, V_2, and V_3 are the respective volumes fractions. Percentage relative density which gives information about the extent of densification was obtained by the below-mentioned formula (H. Naceur, et al. 2014).

$$\text{Density } \% = \frac{\text{Actual Density}}{\text{Theoretical Density}} \times 100 \qquad (4.4)$$

The extent of sintering was obtained by finding the values of actual density and comparing them with the percentage relative density value.

4.4.2 Mechanical characterization

To estimate the mechanical properties of the composite synthesized, different mechanical testings were performed using different instruments. It is to be noted that the specimens required for compression tests were cylindrical and that for flexural testing bar shaped samples were used.

4.4.2.1 Hardness

Hardness is a surface property, which provides the ability to resist localized permanent deformation (Y.T. Cheng and C. M. Cheng, 2000). It can also be defined as the resistance against indentation, penetration, and abrasion. When an external force is applied, the material shows some resistance and this resistance against permanent shape change is known as hardness. From the 'Metals Handbook,' hardness is defined as "Resistance of a metal to plastic deformation, usually by indentation." However, the term may also refer to stiffness or temper or resistance to scratching, abrasion, or cutting. The high hardness of the metal shows high resistance to deformation.

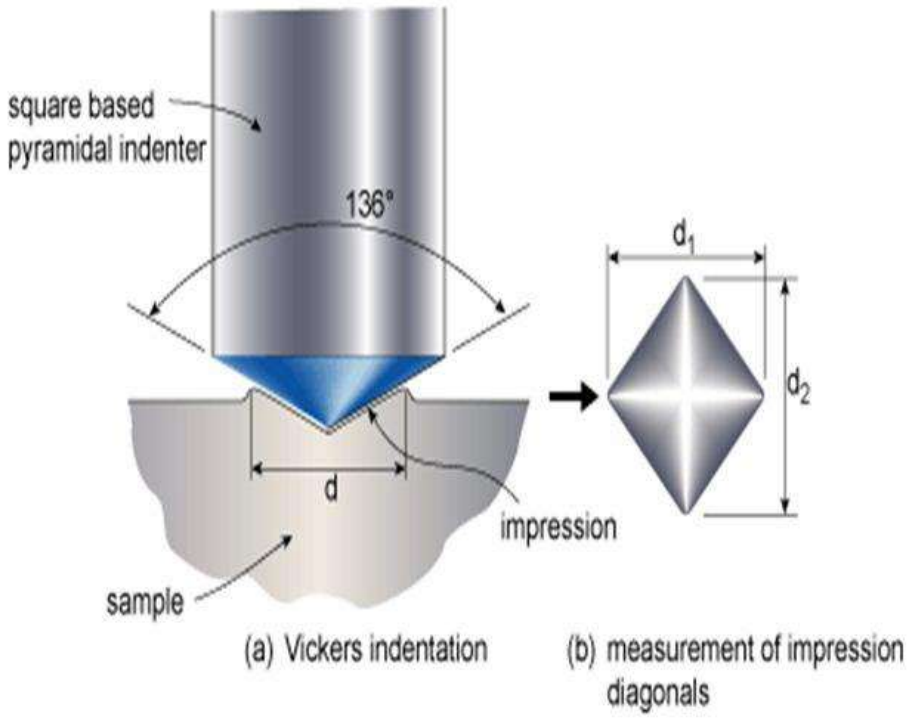

FIGURE 4.17: Vicker's hardness technique used for hardness measurement (H. Ismaeel, et al. 2016)

Different methods such as Shore Hardness Test, Barcol's hardness test, Rockwell Hardness Test, Brinell hardness, Knoop hardness Test, and Vickers Hardness Test are commonly used for the measurement of the hardness worldwide. Fig. 4.17 shows the schematic of the Vickers hardness measurement technique used in the present investigation.

Vickers hardness test is a standard method used for measuring the hardness of metals, particularly those with extremely hard surfaces. Vickers hardness is a measure of the hardness of a material, calculated from the size of an impression produced, under a load by a pyramid-shaped diamond indenter. The indenter employed in the Vickers test is a

square-based pyramid whose opposite sides meet at the apex at an angle of 136°. In this test, the surface is subjected to a standard load for a standard length of time through an indenter. The diagonal of the resulting indentation is measured under a microscope, and the Vickers hardness value read from a conversion table (Y. Wan and J. Gong, 2003).

In present work, the hardness of the samples was measured on Vickers hardness testing equipment, measured by a Leco- LV700AT hardness tester under a load 5 kgf, applied for 5 sec. The Vickers hardness equipment is shown in Fig. 4.18

FIGURE 4.18: Vickers's hardness equipment

The specimens for hardness tests were mechanically polished with 1000 and 1200 grit emery papers. The results for hardness tests were obtained by taking an average of values of the indent diagonal in three different regions. The diagonal length of the test samples was measured from SEM images. The hardness of the samples was calculated in the form of Vickers hardness number (HV) from the method as described by ASTM E384.

$$HV = 1.854 \ {}^{F}/_{d^2} \tag{4.5}$$

Where F is the load or force applied to the diamond indenter in kilograms-force, d is the average length of the two diagonals in mm and HV is the Vickers's hardness or hardness number.

4.4.2.2 Young's modulus

Young's modulus is a measure of stiffness or resistance to elastic deformation under a given load. It relates stress to strain (proportional deformation) along an axis or line. The basic principle is that a material undergoes elastic deformation when it is compressed or extended, returning to its original shape when the load is removed. More deformation occurs in a flexible material compared to that of a stiff material. When the material reaches certain stress, the material will begin to deform. It is up to the point where the material's structure is stretching and not deforming. However, if the stress in the material is more than this, the molecules or atoms inside will begin to deform and permanently change the shape of the material. In present work, to calculate Young's modulus non-destructive testing i.e. ultrasonic testing of the samples was done. In this method, the ultrasonic waves are passed through the specimen, the ultrasonic wave velocities of the samples i.e. longitudinal (V_L) and transverse wave (V_T) were recorded.

The velocity measurements for modulus calculation are most commonly made with precision thickness gages (45MG, Olympus, USA) with single element software, or a flaw detector with velocity measurement capability such as the EPOCH series instruments. The instrument to calculate young's modulus as shown in Fig. 4.19.

FIGURE 4.19: Young's modulus NDT testing equipment

For proper bonding between the sample and transducer glycerine and burnt honey were used as bonding materials. Young's modulus (E) of the base material was calculated using the following equation (E. Reufi and I. Thomas, 2016):

$$\text{Young's modulus (E)} = \frac{V_L^2\,\rho\,(1+\sigma)(1-2\sigma)}{(1-\sigma)} \qquad (4.6)$$

Where ρ is the density of the sample material and σ is the Poisson's ratio of the samples. Poisson's Ratio is the ratio of transverse strain to corresponding axial strain on a material

stressed along one axis. The Poisson's ratio of the specimens can be calculated from the equation (E. Reufi and I. Thomas, 2016):

$$\text{Poisson's ratio } (\sigma) = \frac{1-2(V_T/V_L)^2}{2-2(V_T/V_L)^2} \quad (4.7)$$

4.4.2.3 Flexural strength

Flexural strength is the ability of a material to withstand bending forces perpendicular to its longitudinal axis. The resulting stresses are a combination of compressive and tensile stresses. If a composite component is a beam subject to bending, a flexural test is more appropriate. In present work, in order to calculate the flexural strength of the synthesized composites, the flexural strength (bending tests) was performed by three-point bending tests for the samples using the universal testing machine (UTM) H10KL, Tinius Olsen, USA. The UTM used for the testing of flexural and compressive strength is as shown in Fig.4.20.

FIGURE 4.20: UTM machine for mechanical testing

While performing the tests, the crosshead speed was maintained at 0.5 mm/min, the load applied was 10 kilonewtons. The Flexural strength was then calculated according to ASTM C1674-11 equation:

$$\text{Flexural strength } (\sigma) = (3Pl) / (2bd^2) \quad (4.8)$$

Where, P=applied load (N); l= span length of the sample (mm); b= sample width (mm); d=thickness of the sample (mm).

4.4.2.4 Compressive strength

The compressive strength of a material is the capacity of a material or structure to withstand the compressive load. It measures the ability of a material to withstand a compressive load without failure. In the present work, cylindrical samples were used for compressive strength measurement was used for the uni-axial compression test (dimensions discussed in section 4.3.3). The compression test of the cylindrical samples was done on Universal Testing Machine (H10KL, Tinius Olsen, USA). The cylindrical-shaped samples were tested by applying a load, and the values were obtained from the UTM. For performing the tests, a constant cross-head displacement rate of 1 mm/min to obtain a nominal strain rate of 0.003 s^{-1} for the specimens were kept. The values were obtained for three samples at each temperature and their average values were noted.

4.4.3 Electrochemical characterization

These tests were performed to evaluate the electrochemical properties of the composite. In present work, the corrosion properties, ion release estimation and pontiodynamic polarization technique were adopted to study the electrochemical behavior of the composite. In all the cases, the corrosive medium used was simulated body fluid.

4.4.3.1 Preparation of Simulated Body Fluid

It is a fluid prepared in the laboratory, which has the same composition as human body fluid. It is used for testing corrosion behavior of the composites prepared. It provides the physiological media same as the human body fluid and is used to test the in-vitro characteristics of a material. The concentration of human body fluid in terms of its constituents and its percentage is shown in Table 4.4.

TABLE 4.4: Ion concentrations of human blood plasma and SBF (T. Kokubo, et al. 1990)

S.N	Ion Concentration	Human Blood Plasma	SBF
1.	Na^+	142.0	142.0
2.	K^+	5.0	5.0
3.	Mg^{2+}	1.5	1.5
4.	Ca^{2+}	2.5	2.5
5.	Cl^-	103.0	147.8
6.	HCO_3^-	27.0	4.2
7.	HPO_4^{2-}	1.0	1.0
8.	SO_4^{2-}	0.5	0.5

Procedure to prepare SBF

Step 1: Take 500 ml of ion-exchanged and distilled water into one liter in a beaker.

Step 2: Stir the water in the bottle with a magnetic stirrer, and dissolve the reagents one by one in the order as given in Table 4.4. (It is to be noted that next reagent should be added only when the former reagent is dissolved completely).

Step 3: Adjust the temperature of the solution in the bottle at 36.5°C by using a thermometer bath, and adjust pH of the solution at pH 7.40 by stirring the solution and titrating 1N-HCl solution.

Step 4: Adjust the total volume of the solution to one liter by adding ion-exchanged and distilled water and shaking the flask at 20°C. Store the solution in a refrigerator at 5-10°C.

TABLE 4.5: Reagents used to prepare simulated body fluid (T. Kokubo, et al. 1990)

S.N	Reagents	Amount (SBF)
1.	NaCl	8.035g
2.	$NaHCO_3$	0.355g
3.	KCl	0.225g
4.	$K_2HPO_4.3H_2O$	0.231g
5.	$MgCl_2.6H_2O$	0.311g
6.	HCl	39-44 ml
7.	$CaCl_2$	0.292g
8.	Na_2SO_4	0.292g
9.	Tris	6.118g

4.4.3.2 Corrosion tests (weight loss method)

The corrosion tests of any material are performed to know the rate of deterioration of any material in a specific environment. It gives information about the capability of a material to sustain strength for a given interval of time. In the present work, the weight loss method for evaluating the corrosion rate of the samples was used. The medium used for testing the corrosion rate was simulated body fluid.

In present work, to find out the corrosion rate by weight loss, the test specimens i.e. pellets (having dimensions, diameter 15 mm and thickness 4 mm) were immersed in SBF and kept for different time intervals. After immersion, the pellets were removed and washed properly with ethanol solution. After that, the initial and final weight of the specimens was measured with electronic balance. For observations of the samples for their weight loss and electrochemical phenomenon the samples were kept in vacuum oven at a temperature of 37.8°C (digital image as shown in Fig. 4.21.

FIGURE 4.21: Vacuum oven

It is to be noted that after removing the samples from SBF, to measure weight of the samples after immersion, the specimens were cleaned thoroughly with ethanol in order to remove the corrosion products attached to the samples. The samples were cleaned as per ASTM G1 standards. The corrosion rate of the samples was calculated by using below mentioned formula as per ASTM G1standards.

$$\text{Corrosion Rate (CR)} = (W \times K)/ (A \times T \times D) \quad (4.9)$$

Where W=weight loss of the sample in grams, K=a constant having value 8.76×104, A=area exposed in cm^2, T=time of exposure in hours, D=density in g/cm^2

4.4.3.3 Corrosion tests (potentiodynamic method)

The test was performed on an SP-150 Biologic electrochemical cell having three electrodes connected to Biologic Instrument Potentiostat/Galvanostat. Fig. 4.22 shows the schematic of experimental setup used for corrosion test. It includes a potentiostat, three electrodes cells and a monitor for recording the data. Fig. 4.23 shows three neck cell used for electrode mounting during the test. Each part of the cell is mentioned in this schematic.

FIGURE 4.22: Schematic layout of experiment setup used for corrosion test by potentiodynamic method

In present work it was done by dipping the samples at room temperature in a beaker containing150 mL SBF solution. Before starting measurements, the electrodes were kept in electrolytic solution for around one hour to get stabilized and to obtain open circuit

potential (OCP). Potentiodynamic polarization curves were recorded with respect to OCP in the range -250 to +250mV.

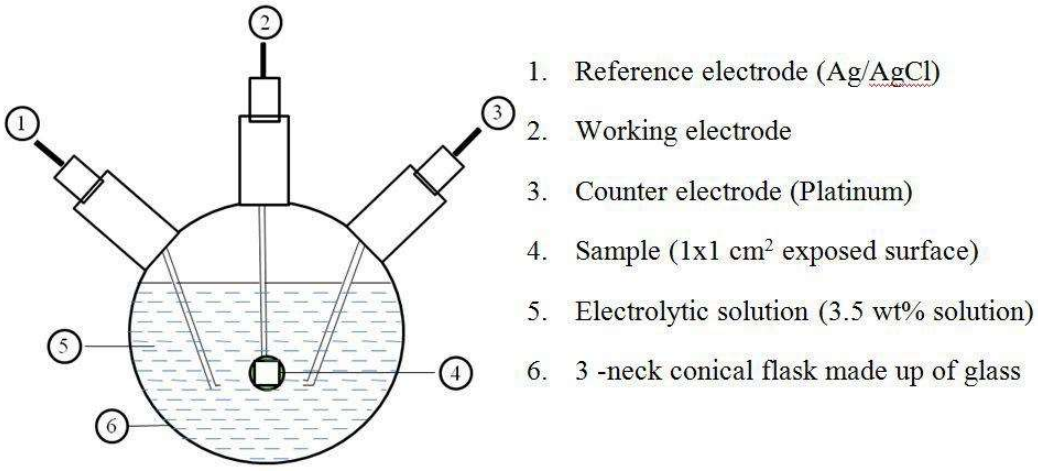

FIGURE 4.23: Schematic of the three neck cell used for electrodes mounting

The tests were performed at a scan rate of 1 mV/s and the polarization curves were obtained and curve fitting was done by Tafel extrapolation techniques for linear fit which gives the values of corrosion potential (Ecorr) and corrosion current density (Icorr) (Y. Liu, et al. 2019). The values of the corrosion current and corrosion potential were used to evaluate corrosion rate of the composites. The extrapolation of both the regions is explained according to the Fig. 4.24.

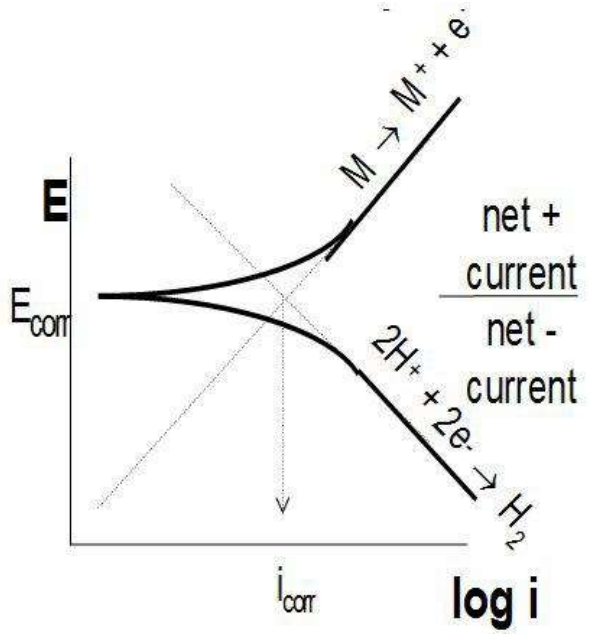

FIGURE 4.24: Tafel extrapolation technique for finding corrosion parameters (R. Ramachandran and M. Nosonovsky, 2015)

4.4.3.4 Atomic absorption spectroscopy (Ion release estimation)

Atomic absorption spectroscopy (AAS) is the method for determination of amount of chemical elements present or number of ions of an element present in a solution, using the absorption of optical radiation by free atoms of the elements in the gaseous state (V. Kuban, et al. 1990). The technique works on the principle that free atoms (in the form of gas) generated in an atomizer can absorb radiation at particular frequency. AAS quantifies the absorption of ground state atoms of the elements in the gaseous state. The atoms transits to higher energy state by absorbing the ultraviolet or visible light. The concentration of the samples in the solution is determined from the amount of absorption in the fluid in parts per million. The instrument was first calibrated using different standards solutions of known concentration. After calibration of the instrument a

calibration curve is generated to determine the unknown concentration of an element in a solution. The solution containing the dipped samples is fed into the instrument, and the absorbance of the element in this solution is recorded. The unknown concentration of the element in the solution is then calculated from the calibration curve directly.

FIGURE 4.25: Atomic absorption spectroscopy setup

In the present case, magnesium is used as the base metal therefore the amount of Mg in the solution may increase considerably with time and hence it is done to estimate the concentration of magnesium ions dissolved in the SBF. The AAS of the samples was done on SHIMADZU AA-7000 atomic absorption spectrophotometer (C. Yafa, and J.G. Farmer, 2006). It should be noted that special precautions were taken during the test as the suction pipe of the spectrophotometer is prone to choking and hence the testing fluid must be filtered properly. For filtration of the fluid, filter paper of diameter 125 mm, 42 numbers were used.

4.4.3.5 Fourier-transform infrared spectroscopy (FTIR)

The most useful tool for identifying chemicals, organic or inorganic, is FTIR spectroscopy. This tool can be used to analyze materials in liquids, solids, and gases. The characteristic of the chemical bond can be detected from the wavelength of the absorbed light as can be seen in the spectrum. The chemical bonds of the molecule can be determined by studying the infrared absorption spectrum. Each pure compound has a unique FTIR spectrum that is called a fingerprint. Although the spectrum of organic material is vibrant and detailed, inorganic compounds have simple absorption spectra. Therefore, the unknown materials can be identified by comparison of their spectrum to a library of known compounds. The FTIR machine that is used was Fourier transform-infrared (FT-IR) spectrometer (1650: Perkin Elmer, Waltham, MA). The absorption bands between 280 to 400 cm^{-1} can be detected by this machine which gives us the ability to identify two of the absorption bands of the composite. Fig. 4.26 shows the FTIR setup.

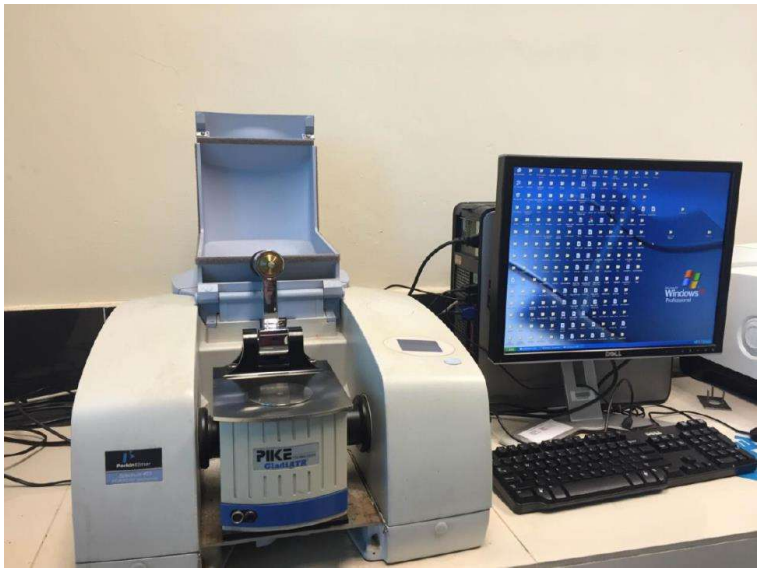

FIGURE 4.26: FTIR measurement set up

In the FTIR mostly molecules of samples absorb light in the infrared region of the electromagnetic spectrum which basically represents the bond of the molecules. The FTIR spectrum is measured in the range of 400-4000 cm^{-1}.

4.4.4 Biological testing

These tests are used to study the property of a material in a biological medium. It studies the response of a particular material towards biological cells. It studies whether the response of a material is neutral or toxic in case of biological interactions. Following tests are the part of biological tests.

4.4.4.1 Cell lines and Cell culture

K562 cells were obtained from ATCC, Manassas, USA. Murine lymphoma cell line DL and the other cells lines were cultured and maintained in complete RPMI-1640 plus supplements including 10% FBS plus antibiotics as described earlier. DL is a spontaneous murine lymphoma and was also maintained in the peritoneum with periodic transfer of the tumor cells to female BALB/c mice.

4.4.4.2 Cell viability assay

Effect of 0% 1393BAG, 10% 1393 BAG, 15% 1393 BAG and 20% 1393 BAG on the viability of tumor cells or normal human cells was evaluated by a colorimetric XTT (sodium 3-[1-(phenylaminocarbonyl)-3,4-tetrazolium]-bis(4-methoxy-6-nitro) assay (Roche, Indianapolis, IN). Tumor cells, normal human peripheral blood mononuclear cells (lymphocytes and monocytes) were plated (5×10^3 cells/well) in 96-well culture dish and incubated with different concentrations of the above-mentioned compounds and incubated at 37^0C, 5% CO_2 for 18 hours. Optical density (OD) was taken at 450 nm in a plate reader

(Synergy HT, BioTek, USA). The percent viable cell was calculated employing the formula below.

$$\% \text{ Cell Viability} = \frac{\text{Experimental } OD_{450}}{\text{Control } OD_{450}} \times 100 \qquad 4.10$$

4.4.4.3 *Cell growth inhibition assay*

Growth inhibitory potential by the compounds against tumor cell was studied by MTT assay. Tumor target cells (5×10^3 cells /well) in a 96 well culture dish were treated with serial concentrations of the compounds. Following incubation at 37^0C, 5% CO_2, for 48 hours, the proliferation of tumor cells was assessed by MTT assay using CellTiter 96 kit (Promega, USA). The measurement of absorbance (OD value) was made at 570 nm in a plate reader (BioTek, USA). Percent inhibition of tumor cells was calculated using under mentioned formula.

$$\% \text{ Growth Inhibition} = [1-\frac{\text{Experimental } OD_{570}}{\text{Target } OD_{570}}]\times100 \qquad 4.11$$

Where experimental OD value indicate the values of tumor cells in the presence of the indicated formulations and Target OD indicate the corresponding values of tumor cell alone, cultured in medium only.

4.4.4.4 Cytotoxicity assay

The lytic activity of 0% 1393 BAG, 10% 1393 BAG, 15% 1393 BAG and 20 % 1393 BAG against tumor cells and normal human cells was measured by cytotoxicity assay using the CytoTox 96 Cytotoxicity assay kit from Promega, USA. Tumor target cells (5×10^3) were co-cultured with varying concentrations of the indicated formulations in a 96

well culture dish. The culture dish was incubated for 18 hours at 37°C, 5% CO_2. Percent-specific lysis was determined from the under mentioned formula.

$$\% \text{ Cytotoxicity} = \frac{(\text{Experimental - Effector Spontaneous - Target Spontaneous})}{(\text{Target Maximum - Target Spontaneous})} \times 100 \qquad 4.12$$

4.4.4.5 Hemolysis assay

For concentration dependent kinetics, the blood sample was incubated with varying concentrations (10-250 μM) of 0 % 1393 BAG, 10% 1393 BAG, 15 % 1393 BAG and 20% 1393 BAG for 4 hours. Hemolysis assay was performed according to the standard protocol. In brief, an aliquot of each blood sample was centrifuged for 5 minutes. 25 μL plasma aliquot was diluted with 225 μL Drabkin's reagent (Sigma) in a 96-well plate and mixed for 2 minutes under lateral agitation (300 rpm). After 10 minutes equilibration at room temperature, optical density was recorded at 540 nm in Synergy HT Multi-Mode Microplate Reader BioTek, USA. Blood haemoglobin was determined by measuring the absorbance of 100-fold dilution of the whole blood in Drabkin's reagent at 540 nm. Saponin (2 mg/mL final blood concentration) and PBS were used as positive and negative control, respectively. A sample of plasma without additives was considered as basal conditions. The standard calibration curve was obtained with the solution containing 0.07–3.8 mg/mL bovine haemoglobin (Sigma) treated with a Drabkin's reagent. The results were presented as percent haemolysis indicating the free plasma haemoglobin (mg/mL) and was measured as released haemoglobin divided by the total blood haemoglobin (mg/mL) multiplied by 100. All measurements were performed in triplicate.